The EMBO Journal Vol.16 No.18 pp.5520–5530, 1997

Essential functions and actin-binding surfaces of yeast cofilin revealed by systematic mutagenesis

Pekka Lappalainen, Elena V.Fedorov[1], Alexander A.Fedorov[1], Steven C.Almo[1] and David G.Drubin[2]

Department of Molecular and Cell Biology, 401 Barker Hall, University of California, Berkeley, CA 94720 and
[1]Department of Biochemistry, Albert Einstein College of Medicine, 1300 Morris Park Avenue, Bronx, NY 10461, USA

[2]Corresponding author
e-mail: drubin@mendel.berkeley.edu

Cofilin stimulates actin filament turnover *in vivo*. The phenotypes of twenty yeast cofilin mutants generated by systematic mutagenesis were determined. Ten grew as well as the wild type and showed no cytoskeleton defects, seven were recessive-lethal and three were conditional-lethal and caused severe actin organization defects. Biochemical characterization of interactions between nine mutant yeast cofilins and yeast actin provided evidence that F-actin binding and depolymerization are essential cofilin functions. Locating the mutated residues on the yeast cofilin molecular structure allowed several important conclusions to be drawn. First, residues required for actin monomer binding are proximal to each other. Secondly, additional residues are required for interactions with actin filaments; these residues might bind an adjacent subunit in the actin filament. Thirdly, despite striking structural similarity, cofilin interacts with actin in a different manner from gelsolin segment-1. Fourthly, a previously unrecognized cofilin function or interaction is suggested by identification of spatially proximal residues important for cofilin function *in vivo*, but not for actin interactions *in vitro*. Finally, mutation of the cofilin N-terminus suggests that its sequence is conserved because of its critical role in actin interactions, not because it is sometimes a target for protein kinases.

Keywords: actin/cofilin/mutagenesis/yeast

Introduction

A remarkable feature of the actin cytoskeleton is its dynamics. In migrating fibroblasts and in the comet tail of a *Listeria* bacterium, actin filaments elongate and shorten with assembly and disassembly rates of up to 9 μm/min (Theriot and Mitchison, 1991; Theriot *et al.*, 1992). These rates are about two orders of magnitude higher than the rate of actin filament disassembly *in vitro* (Pollard, 1986). Therefore, cellular factors must stimulate the rapid turnover of the actin cytoskeleton in living cells.

Cofilin and actin depolymerizing factor (ADF) are two members of a family of small (15–20 kDa) actin-binding proteins. All eukaryotic cells appear to have at least one member of this family (for review see Moon and Drubin, 1995). Cofilin/ADF proteins typically localize to regions of cells characterized by high actin dynamics, including neuronal growth cones, ruffling membranes, cleavage furrows and yeast cortical actin patches (Bamburg and Bray, 1987; Yonezawa *et al.*, 1987; Moon *et al.*, 1993; Nagaoka *et al.*, 1995). Recent studies have shown that cofilin/ADF proteins play a central role in stimulation of actin dynamics in the *Listeria* tail in cell extracts (Carlier *et al.*, 1997; Rosenblatt *et al.*, 1997) and in the cortical actin cytoskeleton in living yeast cells (Lappalainen and Drubin, 1997). Mutations that inactivate cofilin/ADF in *Caenorhabditis elegans*, *Drosophila melanogaster* and *Saccharomyces cerevisiae* are lethal, indicating that the activity of these proteins is fundamentally important for eukaryotes (Moon *et al.*, 1993; McKim *et al.*, 1994; Gunsalus *et al.*, 1995).

Cofilin/ADF proteins bind to both G- and F-actin with high affinity ($K_d < 1$ μM) and are able to stimulate actin filament depolymerization *in vitro* (Carlier *et al.*, 1997). The actin depolymerization activity of cofilin is regulated by pH, being favored in an alkaline environment (pH > 7.2) (Yonezawa *et al.*, 1985; Hawkins *et al.*, 1993; Hayden *et al.*, 1993). The association of cofilin/ADF with actin can be inhibited by phosphoinositides (Yonezawa *et al.*, 1989a; 1991a) and by phosphorylation (Morgan *et al.*, 1993). Electrospray mass spectroscopy and site-directed mutagenesis studies have identified Ser3 as a target of phosphorylation in chicken ADF (Agnew *et al.*, 1995), suggesting that this residue may be located near/at the actin-binding site of this protein.

The recent NMR structure of a cofilin homolog, destrin (Hatanaka *et al.*, 1996), together with the crystal structures of yeast cofilin and *Acanthamoeba* actophorin (Fedorov *et al.*, 1997; Leonard *et al.*, 1997) provide an opportunity to develop a deeper understanding of the molecular mechanism by which these proteins stimulate F-actin turnover *in vivo*. However, relatively little is known about the actin-binding surface(s) of cofilin. In addition to implication of the N-terminal serine (Ser3) described above in actin-binding, site-directed mutagenesis studies have suggested that Lys112 and Lys114 in porcine brain cofilin are important for F-actin binding and depolymerization (Moriyama *et al.*, 1992). Based on structural homology to a segment of gelsolin, it was suggested that cofilin might interact with actin in a manner similar to that of gelsolin segment-1 (Hatanaka *et al.*, 1996). An atomic model of gelsolin segment-1–actin monomer complex has been reported (McLaughin *et al.*, 1993). However, the poor conservation of residues between cofilin and gelsolin segment-1 at the putative actin-binding region raises questions about the validity of this hypothesis. Therefore, identifying the actin-binding region of cofilin either by systematic mutagenesis or by structural approaches is essential for elucidating the mechanism of cofilin/actin interactions.

Table I. Growth phenotypes of the yeast cofilin mutants

Mutations	Allele	Growth phenotype	Actin organization	Detection
Wild type	*COF1*	wt (14–37°C)	+	
D10A, E11A	*cof1-5*	ts$^-$ (14–25°C)	–	*Hin*fI
D18A, K20A	*cof1-6*	wt	+	*Nsi*I
K23A, K24A, K26A	*cof1-8*	ts$^-$ (14–30°C)	–	*Bbv*I
D34A, K36A, E38A	*cof1-9*	lethal (recessive)	n.d.	*Bbv*I
K42A, E43A	*cof1-10*	wt	+	*Bbv*I
D47A, D51A	*cof1-11*	wt	+	*Bbv*I
E55A, K56A	*cof1-12*	wt	+	*Bbv*I
E59A, D61A	*cof1-13*	wt	+	*Alu*I
D68A, E70A, E72A	*cof1-14*	lethal (recessive)	n.d.	*Rsa*I
E77A, K79A	*cof1-15*	wt	+	*Mae*I
R80A, K82A	*cof1-16*	lethal (recessive)	n.d.	*Bst*UI
R96A, K98A	*cof1-17*	lethal (recessive)	n.d.	*Bgl*II
K105A, D106A	*cof1-18*	wt	+	*Bbv*I
R109A, R110A	*cof1-19*	wt	+	*Bbv*I
D123A, E126A	*cof1-20*	lethal (recessive)	n.d.	*Bst*UI
D130A	*cof1-21*	wt	+	*Bst*UI
E134A, R135A, R138A	*cof1-22*	ts$^-$ (14–25°C)	–	*Bbv*I
S4A	*cof1-4*	wt	±	*Bgl*II
S4E	*cof1-3*	lethal (recessive)	n.d.	*Bgl*II
M1–G5 deletion	*cof1-28*	lethal (recessive)	n.d.	

Amino acid changes, allele numbers and defects in growth and actin organization are listed. The temperature range over which a strain was able to grow is indicated in parentheses. The restriction endonucleases that were used to confirm the mutations are shown.

Identification of a cofilin homolog in the yeast *S.cerevisiae* has opened new avenues for studying the function of this small actin-binding protein (Iida *et al.*, 1993; Moon *et al.*, 1993). Because cofilin is an essential gene, it is possible to use yeast molecular genetics to identify cofilin residues that are important for cofilin–actin interactions. Systematic mutagenesis approaches combined with yeast genetics have been successfully applied to identify functional domains in other essential cytoskeletal proteins such as actin and β-tubulin (Wertman *et al.*, 1992; Reijo *et al.*, 1994). Here, we have combined systematic mutational analysis of the yeast *COF1* gene and biochemical characterization of mutant cofilins. This approach allowed us to identify residues that are required for cofilin function *in vivo* and to analyze the biochemical defects of these cofilin alleles. The mapping of these residues onto the three-dimensional structure of yeast cofilin implicates distinct molecular surfaces of cofilin in F-actin- and G-actin-related functions.

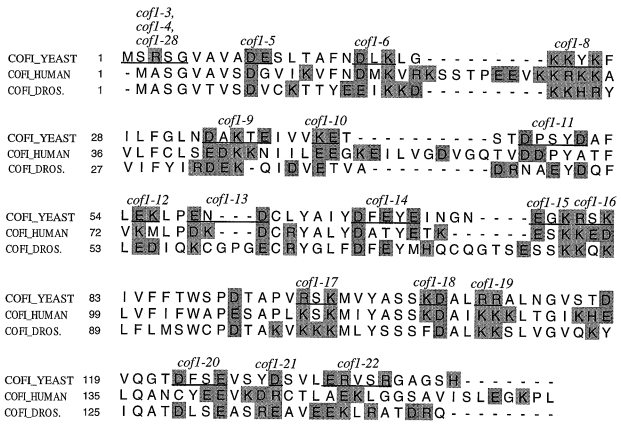

Fig. 1. Alignment of amino acid sequences of yeast (*S.cerevisiae*), human and fruitfly (*D.melanogaster*) cofilins (Ogawa *et al.*, 1990; Moon *et al.*, 1993a; Gunsalus *et al.*, 1995). The charged residues (Lys, Arg, His, Glu and Asp) are highlighted. The residues that were mutated are underlined and the corresponding allele numbers are indicated above the sequence.

Results

Site-directed mutagenesis strategy

The overall goal of our analyses was to identify by mutagenesis regions in yeast cofilin that are important for function *in vivo*, and to elucidate the biochemical defects of the resulting mutants. We wished to discover mutations that impaired protein–protein interactions rather than protein stability. Since our mutagenesis was initiated prior to determination of the molecular structure of cofilin, we used a 'clustered-charged-to-alanine' strategy (Bass *et al.*, 1991; Wertman *et al.*, 1992) to bias mutations to the surface of the protein. Whenever two or more charged residues were present in a window of five residues, the charged residues were changed to alanines. Each mutant allele contained one to three amino acid substitutions (Table I). The alignment of *S.cerevisiae*, *D.melanogaster* and human cofilins, together with the amino acid changes of the 17 charged-to-alanine substitutions, are shown in Figure 1. In addition to the charged-to-alanine mutations, we replaced Ser4 with alanine (*cof1-4*) and glutamate (*cof1-3*). This serine corresponds to a residue that is phosphorylated in more complex eukaryotes (Agnew *et al.*, 1995). The serine-to-alanine mutation was intended to encode constitutively unphosphorylated cofilin, whereas the glutamate substitution was intended to mimic the phosphorylated state. Finally, to test the importance of the first five residues, which are disordered in the recently determined crystal structure of yeast cofilin (Fedorov *et al.*, 1997), we also created a yeast cofilin allele (*cof1-28*) missing residues two to five.

Oligonucleotide-directed mutagenesis was carried out as described in the Materials and Methods. For all mutations, the oligonucleotide sequence was designed to make the mutation verifiable by restriction digest (see

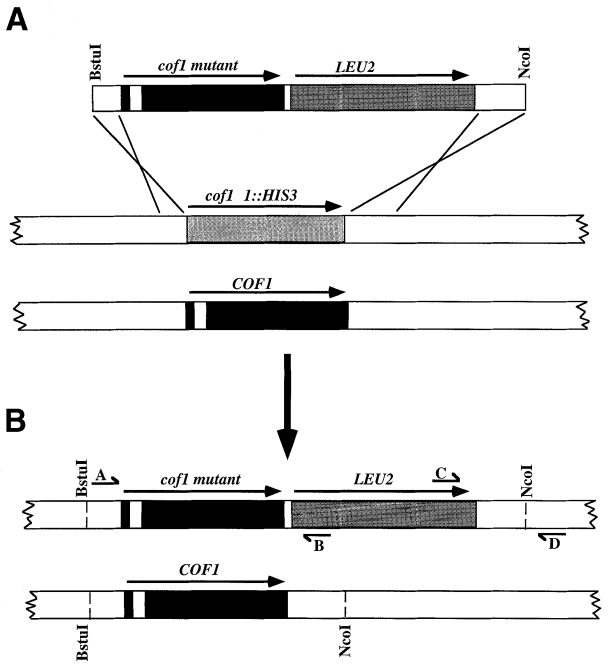

Fig. 2. Strategy for *cof1*-mutant integration. A *Bst*UI–*Nco*I fragment carrying a cofilin mutant gene linked to *LEU2* was integrated into the genome of a diploid strain heterozygous for the *cof1Δ1::HIS3* deletion. The desired integration [crossovers indicated in (**A**)] results in the configuration shown in (**B**), and a Leu^+ His^- phenotype. Upon sporulation and tetrad dissection, the phenotypes of the cofilin mutants (Leu^+ segregants) were determined. Oligonucleotides A and B [shown in (B)] were used for amplification of the cofilin gene for the subsequent analytical restriction enzyme digestion to confirm the presence of the correct mutation in the genome. Oligonucleotides C and D were used for confirming that the *cof1* alleles were integrated into the correct position of the genome. Note that oligonucleotide D is located outside the integrated region.

Table I). Most of the mutations introduce a new restriction site. However, *cof1-3*, *cof1-4* and *cof1-17* destroy *Bgl*II sites. All mutations were verified at the plasmid stage by restriction digestions and subsequent DNA sequencing (data not shown).

Chromosomal integration of mutant cofilin genes in yeast diploids

All *cof1* alleles were expressed in single copy at the *COF1* chromosomal locus. The plasmid in which the mutagenesis was performed contains the entire *COF1*-coding sequence linked to the *LEU2* gene, which was inserted 91 bp downstream of the *COF1* translational terminator. In this plasmid, *COF1* and *LEU2* are transcribed in the same direction. *LEU2* provided a selectable marker for the integration of the *cof1* alleles (Figure 2). Strains expressing wild-type *COF1* linked to *LEU2* at the *COF1* chromosomal locus grow normally at all temperatures tested (14–37°C) (Table I) and have normal actin and cofilin organization (data not shown).

Plasmids carrying the *cof1* mutant alleles were linearized as described in the Materials and methods. The linearized *cof1-LEU2* fragments were transformed into a diploid strain carrying a disruption of *COF1* (*cof1-Δ1::HIS3*). By screening among the Leu^+ transformants for those that were also His^-, it was insured that the *cof1-Δ1::HIS3* allele was replaced with the *cof1::LEU2* from the plasmid. This also insured that the entire *cof1* mutant allele was integrated, because recombination was forced to occur outside the cofilin open-reading-frame (strategy adapted from Wertman *et al.*, 1992). The presence of the desired mutations, and integration at the *COF1* chromosomal locus, were verified by polymerase chain reaction amplification of the genomic DNA and subsequent restriction endonuclease digestions as described in Materials and methods.

In vivo phenotypes of cof1 mutants

None of the mutations created in this work resulted in a dominant-lethal phenotype. Therefore, the mutant phenotypes were analyzed in haploid segregants. For each cofilin mutant, cells from two Leu^+/His^- transformants were sporulated and at least six tetrads were dissected and germinated on rich medium at 20°C. Five charged-to-alanine alleles as well as the Ser4Glu mutant and the N-terminal deletion showed 2:2 segregation of viability: nonviability and all viable segregants were Leu^-. These mutations are therefore concluded to result in recessive lethality (Table I). Three mutants (*cof1-5*, *cof 1-8* and *cof1-22*) showed temperature sensitivity for viability. *cof1-5* and *cof-8* formed colonies of normal size between 14°C and 25°C, or 14°C and 30°C, respectively, but were inviable at temperatures >30°C. *cof1-22* showed normal growth between 14°C and 25°C and grew very slowly at temperatures between 25°C and 37°C. Other *cof1* alleles, including the Ser4Ala mutation, showed similar growth to the wild-type *COF1* allele over all temperatures examined (14–37°C).

For the non-lethal *cof1* alleles, actin organization was examined by fluorescence microscopy using rhodamine–phalloidin. We found that in the conditional-lethal alleles (*cof1-5*, *cof1-8* and *cof1-22*) actin organization was severely altered at the non-permissive temperature (Lappalainen and Drubin, 1997). In contrast, the alleles that showed wild-type growth properties showed actin organization indistinguishable from that of the wild type (see Table I). The one exception was *cof1-4* which showed slightly aberrant actin organization (data not shown) despite having wild-type growth properties.

Biochemical properties of the mutant proteins

In order to determine the biochemical defects that are responsible for the lethal and temperature-sensitive phenotypes observed in yeast, we expressed all such *cof1* mutants in *Escherichia coli* and purified the recombinant proteins. In addition to these mutants, as a control, we expressed in *E.coli* Cof1-12 (E55A, K56A), an allele for which no phenotype was detected in yeast. With one exception (see below) mutant proteins were expressed as glutathione-*S*-transferase (GST) fusion proteins in the pGEX.2T vector (see Materials and methods). The fusion proteins were purified on glutathione–agarose, cofilin was cleaved from GST by thrombin digestion, and the two resulting proteins were separated from each other by gel filtration. The thrombin cleavage site introduces two additional residues (glycine followed by serine) at the N-terminus of the recombinant proteins. In full-length cofilin, this results in replacement of the N-terminal methionine by glycine. In the Met1–Gly5 deletion this would result in a replacement of Val6 and Ala7 by glycine and serine, respectively. Therefore, this mutant

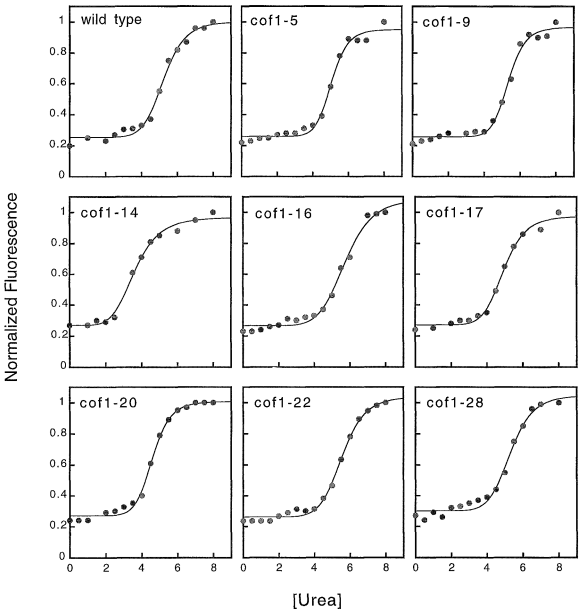

Fig. 3. The stability of the recombinant proteins measured by fluorescence-monitored urea denaturation as described in Materials and methods. The arbitary fluorescence units are shown on the *y*-axis and the urea concentration on the *x*-axis. Note that Cof1-14 unfolds at a significantly lower urea concentration than wild-type cofilin.

(Cof1-28) was instead expressed in *E.coli* as a non-fusion protein in the pBAT4 vector (see Materials and methods). This results in a recombinant protein with an identical N-terminal sequence to the corresponding yeast cofilin allele (*cof1-28*).

Recombinant wild-type and mutant cofilins, except for Cof1-14 (D68A, E70A, E72A), showed similar levels of expression in *E.coli*. The Cof1-14 allele was expressed at approximately one-fifth of the wild-type level, which may be a result of protein degradation. The elution profiles obtained using a Superdex-75 gel-filtration column suggest that wild-type cofilin and most cofilin mutants behave as monomers at neutral pH. However, >95% of Cof1-8 (K23A, K24A, K26A) elutes from this column in the void volume, suggesting the formation of aggregates. After purification by gel filtration, wild-type cofilin, as well as all of the mutants, were >99% pure, based on inspection of Coomassie-stained SDS gels (data not shown).

To determine the effects of specific mutations on the overall stability of the cofilin molecules, fluorescence-monitored urea denaturation was performed on each recombinant protein (Figure 3). The behavior of the wild-type and mutant cofilins is consistent with a simple two-state unfolding transition. The wild type and most of the mutants, including the N-terminal deletion, show a mid-point for the transition at ~5.3 M urea, indicating that these mutations do not significantly perturb the stability of cofilin. The mutant Cof1-20 (D123A, E126A) is slightly less stable (4.7 M), while Cof1-14 (D68A, E70A, E72A) is significantly less stable than the wild type (3.6 M). These data indicate that residues Asp68, Glu70 and/or Glu72 contribute to the stability of cofilin. However, it is important to note that this urea denaturation assay measures only the folded to unfolded transition of the entire cofilin molecule. Therefore, it is possible that some of our charged-to-alanine mutations result in local conformational changes which are not detected by monitoring tryptophan fluorescence during urea denaturation.

The interaction of yeast mutant cofilins with yeast actin filaments was first studied by use of a co-sedimentation assay. Recombinant yeast cofilins and pre-polymerized yeast actin were mixed to a final concentration of 2 μM each. After incubation for 60 min at room temperature, the actin filaments were sedimented by centrifugation, and the amount of actin and cofilin in the pellets and supernatants was quantified by densitometry of Coomassie-stained SDS gels (see Materials and methods). A representative gel from a co-sedimentation assay is shown in Figure 4A, and quantified data for all mutants are presented in Figure 4B. While Cof1-12 (E55A, K56A) (control), Cof1-5 (D10A, E11A) and Cof1-9 (D34A, K36A, E38A) did not show a detectable decrease in F-actin binding, all other mutants showed a variable range of defects in actin filament binding (Figure 4B). Mutants that showed defects in F-actin binding in this assay (Figure 4B) were analyzed further by co-sedimentation using a range of F-actin concentrations (Figure 4C). Cof1 (wild type) shows saturation of binding at 4 μM actin. Cof1-22 and Cof1-20 bound to actin filaments more weakly at all actin concentrations, but the binding increased in a concentration-dependent manner, suggesting that the binding is saturable. In contrast, Cof1-16, Cof1-17 and Cof1-28 show no significant increase in binding within the F-actin concentration range tested (0–6 μM), indicating that these mutants bind to F-actin with very low affinities.

The ability of the mutant cofilins to interact with actin-ATP monomers was assessed by native gel electrophoresis of cofilin–actin complexes and by inhibition of nucleotide exchange by the actin monomer. Formation of the cofilin–G-actin complex has been shown to inhibit nucleotide exchange by the actin monomer (Hawkins *et al.*, 1993). The results from these two assays were entirely consistent in that both implicated the same alleles as being defective in monomer binding. However, as the detection of cofilin–actin monomer complexes from native gel electrophoresis is complicated by the mobility shifts caused by charged-to-alanine mutations, only the data from the nucleotide exchange assay are shown (Figure 5). Only three mutations (Cof1-17, Cof1-20 and Cof1-28) showed significant defects in actin-ATP monomer binding in these two assays. The Cof1-16 and Cof1-22 mutants that have severe defects in F-actin binding showed only very small defects in G-actin binding, suggesting that the F-actin binding surface of cofilin is more extended than the G-actin binding surface.

We next determined whether the cofilin mutations are defective in F-actin depolymerization. Purified yeast actin was polymerized to a final concentration of 5 μM and was then diluted with buffer containing different cofilins to a final concentration of 0.5 μM cofilin and 0.5 μM yeast F-actin. The depolymerization of actin filaments was followed immediately after dilution by the decrease in light-scattering at 400 nm. As shown in Figure 6, dilution of 5 μM actin filaments to 0.5 μM results in slow depolymerization of the filaments. This depolymerization occurs when the monomeric actin concentration falls below the critical concentration for F-actin assembly, which for ATP-actin is ~0.1 μM (Pollard, 1986). Wild-type cofilin and Cof1-12 (E55A, K56A) (control) promote

a large increase in the actin filament depolymerization rates (Figure 6). All other mutants show variable defects in F-actin depolymerization. However, mutants Cof1-5 (D10A, E11A) and Cof1-9 (D34A, K36A, E38A), both of which bind actin monomers and actin filaments with a similar affinity to the wild-type cofilin, show only minor decreases in stimulation of actin filament depolymerization compared with the wild-type cofilin (Table II), despite showing dramatic defects (temperature sensitivity or lethality, respectively) *in vivo*. Therefore, it is possible that the phenotypes of these two mutants result from a currently unidentified activity of cofilin. It should also be noted that wild-type cofilin expressed as a GST fusion protein in the pGEX2T vector (which results in the replacement of Met1 by glycine), and non-fusion wild-type cofilin expressed in pBAT4 (which maintains Met1), are indistinguishable in all the biochemical assays described above (data not shown). In addition, the mutant Cof1-12 (E55A, K56A), which showed no phenotype in yeast, did not show detectable differences compared with wild-type cofilin in any of our biochemical assays (Table II).

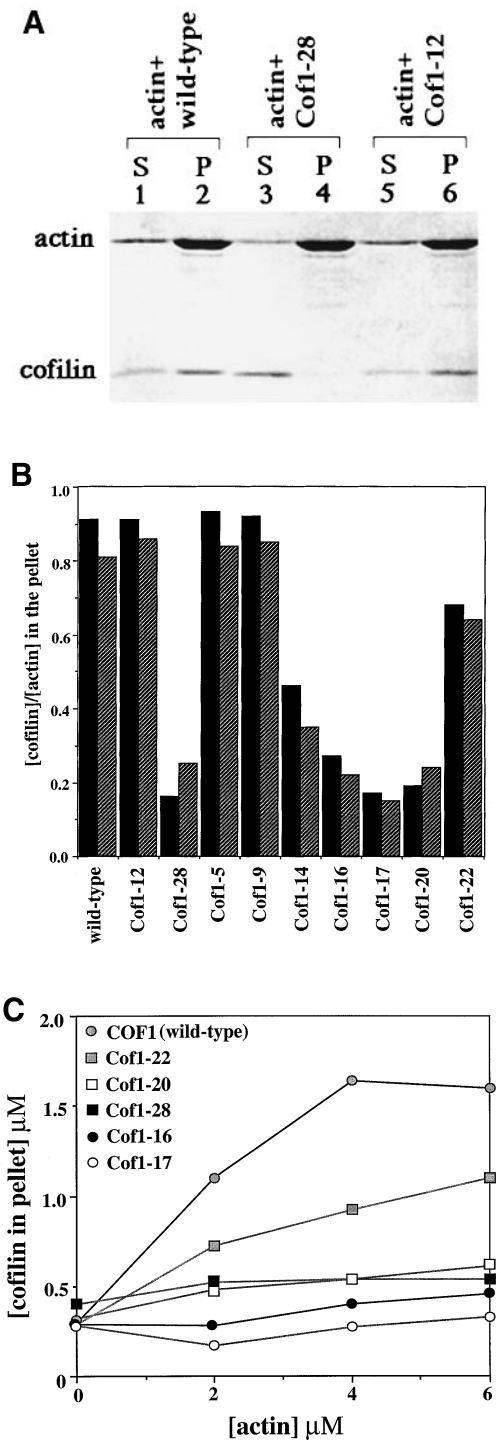

Fig. 4. (**A**) Representative co-sedimentation data. The assay was performed by mixing 2 μM pre-polymerized yeast actin filaments with 2 μM wild-type or mutant cofilin. In the wild-type cofilin sample (lanes 1 and 2, S = supernatant and P = pellet), ~73% of the actin and 67% of the cofilin are found in the pellet. In contrast, only 13% of Cof1-28 (M1-G5 deletion) pelleted. Note that the amount of actin in the pellet for this mutant was higher than for wild-type cofilin (85% for the Cof1-28 mutant compared with 73% for the wild type). Cof1-12, which shows no phenotype in yeast, co-sediments with actin filaments similarly to the wild-type cofilin (lanes 3 and 4). (**B**) The cofilin/actin molar ratios in the pellet from two independent co-sedimentation experiments using 2 μM actin and 2 μM cofilin. Ratios were determined by densitometry of Coomassie-stained SDS-gels like the one shown in Figure 4A. Note that Cof1-5 (D10A, E11A), Cof1-9 (D34A, K36A, E38A) and Cof1-12 (E55A, K56A) show similar affinity for actin filaments as the wild-type cofilin. The other six mutants show variable defects in F-actin binding. (**C**) Co-sedimentation of cofilin/cofilin mutants with 0, 2, 4 or 6 μM actin in F-buffer. The cofilin concentration in these experiments was 2 μM and the concentration of cofilin that co-sedimented with actin filaments is shown on the *y*-axis.

Mapping the cofilin alleles on the three-dimensional structure of yeast cofilin

The three-dimensional structure of yeast cofilin has been determined recently by X-ray crystallography (Fedorov *et al.*, 1997), allowing us to map the mutants generated in this study onto the surface of the cofilin molecule. The charged residues that can be mutated to alanines without a discernible *in vivo* phenotype are mostly clustered on either side of the 'disc-shaped' cofilin molecule (Figure 7, green), while the mutants that result in lethal or temperature-sensitive phenotypes cluster along the circumference of the molecule (Figure 7, red, orange and blue). The residues that are altered in mutants with reduced cofilin stability (Lys23, Lys24, Lys26, Asp68, Glu70 and Glu72) are located proximal to each other (Figure 6, blue). Side chains of Lys23 and Asp68 form a salt bridge, while the side chain of Lys26 forms a hydrogen bond with the main chain carbonyl oxygen of Asp68. This offers a plausible explanation for the folding/stability problems in the Cof1-8 and Cof1-14 mutants. Residues Asp10, Glu11, Asp34, Lys36 and Glu38 (Cof1-5 and Cof1-9), which do not appear to play an important role in F-actin binding or depolymerization, but whose mutation can result in inviability or temperature sensitivity for growth at high temperatures, also cluster close to each other (Figure 7, orange).

The residues that are altered in mutants with markedly decreased F-actin binding and depolymerization form a half-circle along the edge of cofilin (Figure 7, red). Interestingly, only three out of five mutants showing defects in F-actin binding and depolymerization (i.e. Cof1-17, Cof1-20 and Cof1-28, but not Cof1-16 and Cof1-22) also show defects in actin monomer binding. Finally, it is also important to note that the cofilin residues which are

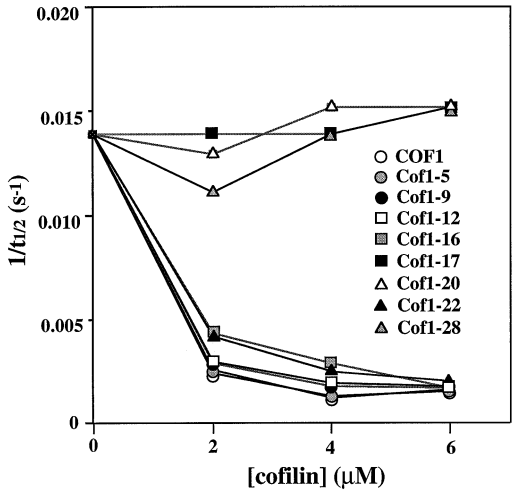

Fig. 5. Interaction of cofilins with G-actin-ATP was determined by the inhibition of actin nucleotide exchange. The reaction rates are indicated on the *y*-axis as the inverse of the reaction half-life ($t_{1/2}$). The final actin concentration for each reaction was 2 μM and the concentrations of cofilins are indicated on the *x*-axis.

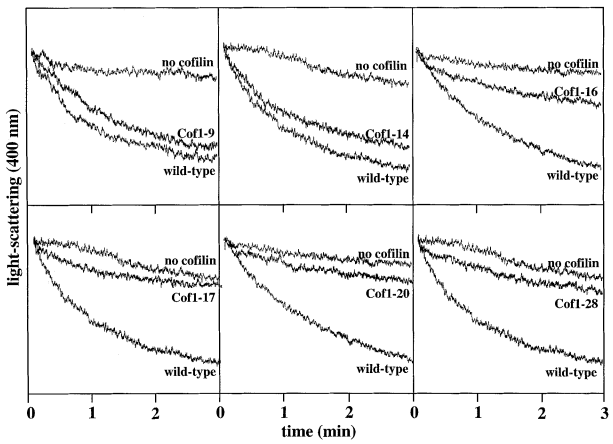

Fig. 6. Representative kinetic data from actin depolymerization assay induced by dilution of F-actin samples. Actin filament depolymerization was followed for 3 min at 25°C by the decrease in light-scattering at 400 nm after dilution of 5 μM F-actin with buffer containing cofilin to final concentrations of 0.5 μM cofilin to 0.5 μM F-actin. The spontaneous depolymerization of F-actin (no cofilin) and F-actin depolymerization stimulated by wild-type cofilin were monitored in parallel for each mutant sample.

not important for protein stability, but which are important for viability and growth at high temperatures, are located close to the most highly conserved, solvent-accessible hydrophobic residues (Figure 7, purple; Val40, Val41, Met99 and Val100). Solvent-exposed hydrophobic residues that are conserved in evolution are in general located in the areas involved in protein–protein interactions (Janin *et al.*, 1988). This provides support for our model, in which these surfaces participate in essential interactions with actin and/or other proteins.

Discussion

The actin-binding surface of cofilin

In a systematic mutagenesis of the yeast *COF1* gene, we generated 20 cofilin mutants. As shown in Figure 7, these mutants are evenly distributed over the surface of yeast cofilin, and therefore represent a significant coverage of the molecular surface. Ten of the cofilin mutations caused either conditional-lethal or lethal phenotypes *in vivo*. Biochemical characterization of mutant cofilins revealed that seven of these mutations decrease actin filament binding and/or depolymerization activity without affecting protein stability (Table II). Previous site-directed mutagenesis studies have shown that Lys112 and Lys114 in porcine cofilin (corresponding to Arg96 and Lys98 in yeast cofilin) are important for F-actin binding and depolymerization activities (Moriyama *et al.*, 1992). Cross-linking studies by Sutoh and Mabuchi (1989) have also implicated the N-terminal segment of destrin (residues 1–20) in interactions with actin. Our studies confirm the role of Arg96 and Lys98 (Cof1-17) and the N-terminal region of cofilin (Cof1-28) in F-actin binding and depolymerization and show that these regions are also essential for G-actin binding. The first five amino acids of yeast cofilin, which are disordered in the crystal structure (Fedorov *et al.*, 1997), are particularly important for these activities (Table II).

Our systematic mutagenesis also revealed that several previously untested regions of cofilin are important for these activities: mutants Cof1-16 (R80A, K82A) and Cof1-22 (E134A, R135A, R138A) show severe defects in actin filament binding and depolymerization, and no detectable defects in G-actin binding. Cof1-20 (D123A, E126A) shows severe defects in inteactions with both F- and G-actin. Mutants Cof1-5 (D10A, E11A) and Cof1-9 (D34A, K36A, E38A) are very interesting because, despite causing severe phenotypes *in vivo*, they show no defects in F- of G-actin binding and show only small defects in F-actin depolymerization *in vitro*. It is possible that the phenotypes of these two mutants result from a currently unrecognized activity of cofilin.

Earlier studies using synthetic peptides to inhibit the cofilin–actin interaction predicted that residues in the middle of the long α-helix of cofilin (122–128 in human cofilin; 106–112 in yeast cofilin) might play an important role in actin filament binding (Yonezawa *et al.*, 1989b). However, our results suggest that the charged residues in this region of yeast cofilin are not critical for the cofilin–actin interaction *in vivo* (see Table I for *cof1-18* and *cof1-19*). One possible explanation for this discrepancy is that the heptapeptide used by Yonezawa *et al.*, (1989b) is highly charged (DAIKKKL) and could therefore interact with actin or cofilin in a non-specific manner. Peptide concentrations in a millimolar range were required to inhibit the cofilin–actin interaction in this study, further suggesting that the peptide–actin interaction might have been non-specific.

Based on the structural homology between cofilin and gelsolin segment-1, it has been hypothesized that cofilin and gelsolin segment-1 might interact with actin in a similar manner (Hatanaka *et al.*, 1996). However, the actin-binding interface of cofilin indentified in our studies is distinct from the actin-binding surface of gelsolin segment-1, identified from a segment-1–actin co-crystal structure (McLaughlin *et al.*, 1993). The F-actin binding site of yeast cofilin maps along an edge of the protein and extends from the N-terminus, across the beginning of the long α-helix to the C-terminus (Figure 8A). A subset of the residues implicated in F-actin binding is also

Table II. Biochemical characterization of temperature-sensitive and lethal yeast cofilin mutants

Mutant	Phenotype	Melting point [urea] (M)	F-actin binding	Depolymerization	G-actin binding
Cof1 (wild type)	wt	5.2	+++	+++	+++
Cof1-12 (control)	wt	n.d.	+++	+++	+++
Cof1-5	ts$^-$	5.2	+++	++/+++	+++
Cof1-8	ts$^-$	(aggregated in *E.coli*)	n.d.	n.d.	n.d.
Cof1-9	lethal	5.4	+++	++/+++	+++
Cof1-14	lethal	3.6	++	++	n.d.
Cof1-16	lethal	5.4	+	+	++/+++
Cof1-17	lethal	5.0	+	+	+
Cof1-20	lethal	4.7	+	+	+
Cof1-22	ts$^-$	5.3	++	++	++/+++
Cof1-28	lethal	5.2	+	+	+

The melting point [urea], F-actin binding, F-actin depolymerization and G-actin binding properties of each mutant are indicated. The scoring for F-actin binding is based on the [cofilin]/[actin] ratio in the pellets as shown in Figure 4B (>80% = +++, 30–80% = ++ and <30% = +). The depolymerization and G-actin binding data tabulated here are derived from experiments shown in Figures 6 and 5, respectively, except that the F-actin depolymerization data for the Cof1-5 and Cof1-22 mutants were taken from Lappalainen and Drubin (1997). Note that Cof1-8 (K23A, K24A, K26A) aggregated when expressed in *E.coli*, and therefore the actin binding and depolymerization assays were not carried out for this mutant. *cof1-12* (E55A, K56A), which shows no phenotype in yeast, is indistinguishable from the wild-type cofilin in our biochemical assays.

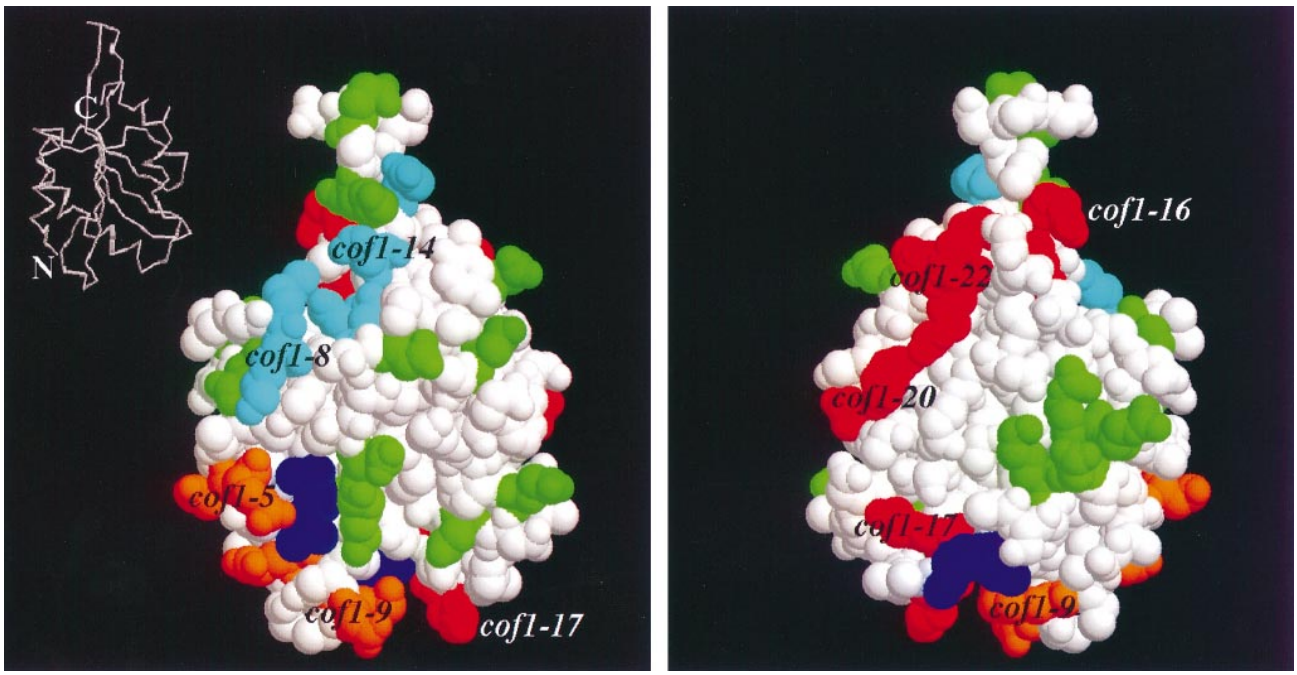

Fig. 7. Space-filling model of the yeast cofilin in two different orientations (rotated 180° horizontally) showing the locations of the cofilin mutations in the three-dimensional structure of cofilin. The residues that can be replaced with alanines without a discernible phenotype in yeast are colored green. The mutations that resulted in altered stability of the protein are shown in blue (*cof1-8* and *cof1-14*). The *cof1-5* and *cof1-9* alleles (orange) do not show defects in stability or F-actin binding, but have small but reproducible defects in the F-actin depolymerization assay. *cof1-16*, *cof1-17*, *cof1-20* and *cof1-22* (red) result in defects in both F-actin binding and depolymerization. Only *cof1-17*, *cof1-20* and *cof1-28* show significant defects in the G-actin binding assay. Note that the residues Met1–Gly5 (Cof1-28), that are disordered in the crystal structure, are probably located close in space to the residues that are mutated in the *cof1-17* allele. The conserved, surface-exposed hydrophobic residues (Val40, Val41, Met99 and Val100) are shown in purple.

important for G-actin binding (Table III). In contrast, the actin-binding site of gelsolin segment-1 is located primarily along and proximal to the long α-helix present in gelsolin segment-1 and cofilin, and the gelsolin residues involved in contacting actin have a different spatial distribution compared with those in cofilin (Figure 8A and B). These results are consistent with the observation that, unlike cofilin, gelsolin segment-1 does not bind to or depolymerize actin filaments (reviewed by Weeds and Maciver, 1993). Cofilin and gelsolin segment-1 show essentially no sequence conservation in the regions that are important for the interaction of gelsolin segment-1 with the actin monomer, further indicating that these two proteins do not interact with actin in similar manner. While gelsolin segment-1 only binds to G-actin, other segments of gelsolin (e.g. segments 2 and 3) bind to F-actin (for review see Weeds and Maciver, 1993). Therefore, it is formally possible that these other segments, which show significant sequence homology and therefore structural homology to segment-1, might interact with F-actin via a binding surface similar to that identified for cofilin.

It is possible that a more extended surface of cofilin is required for F-actin binding than is needed for G-actin binding to allow interactions with neighbouring subunits

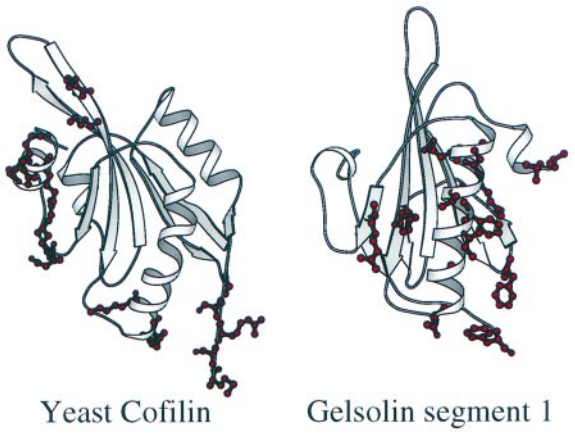

Fig. 8. Ribbon diagrams comparing actin-binding sites of yeast cofilin and gelsolin segment-1. The side-chains of cofilin residues that appear to be important for F-actin binding are indicated by red. The gelsolin residues that are important for G-actin-interaction (right-hand panel, red) are taken from the segment-1–actin monomer co-crystal structure (McLaughin *et al*., 1993).

within actin filaments. This hypothesis is supported by the fact that only three out of five cofilin mutants that showed defects in F-actin binding showed significant defects in our G-actin binding assays (Figure 5 and Table II). These three mutants cluster close to each other around the beginning of the long α-helix. It is possible that when bound to an actin filament, residues mutated in Cof1-17, Cof1-20 and Cof1-28 alleles interact with one monomer, whereas residues mutated in Cof1-16 and Cof1-22 alleles interact with an adjacent monomer in the actin filament.

Function and regulation of cofilin in yeast

Recent studies have shown that members of the cofilin/ADF family stimulate actin filament depolymerization in extracts and *in vivo*, and are key regulators of actin dynamics (Carlier *et al*., 1997; Lappalainen and Drubin, 1997; Rosenblatt *et al.*, 1997). Results from our systematic mutagenesis support the conclusion that cofilin plays an essential role in regulation of actin organization. All three cofilin mutants resulting in a temperature-sensitive phenotype in yeast show severe defects in organization of the actin cytoskeleton. In contrast, cofilin mutants that grew normally at temperatures between 14°C and 37°C did not show severe defects in actin organization (Table I). In addition, since two of our mutants (Cof1-16 and Cof1-22) whose mutations resulted in lethality or temperature sensitivity, respectively, appeared defective in F-actin binding but not G-actin binding, we conclude that the F-actin binding activity cofilin is critical for its essential function. These and other data (Lappalainen and Drubin, 1997) suggest that F-actin binding and stimulation of actin filament depolymerization are essential functions of cofilin in yeast, and most likely in all eukaryotic cells.

Cofilin and ADF are negatively regulated by phosphorylation in many vertebrate cell types (Morgan *et al.*, 1993; Davidson and Haslam, 1994; Saito *et al.*, 1994; Samstag *et al.*, 1996). Phosphorylation of cofilin/ADF sharply reduces its ability to interact with F-actin (Agnew *et al.*, 1995) and may play an essential role in the early stages of development in *Xenopus* (Abe *et al.*, 1996). The replacement of Ser4, which corresponds to the Ser3 in vertebrate cofilin/ADF that can be phosphorylated *in vivo*, by alanine caused no readily detectable phenotype in yeast (Table I). This indicates either that in contrast to vertebrates yeast cofilin is not phosphorylated at this serine, or that phosphorylation does not play an essential role during the haploid life cycle. The inability to detect a phosphorylated form of yeast cofilin (P.Lappalainen, unpublished observations; J.Bamburg, personal communication) supports the former possibility. In light of these results, it is possible that regulation of cofilin by phosphorylation is unique to organisms and cell types in which stimulus-responsive inactivation of actin filament depolymerization is required to stabilize specific actin filament populations. Nevertheless, the lethal phenotype of the Ser4Glu mutation in yeast cofilin suggests that phosphorylation of this residue in yeast would similarly disrupt the interaction between cofilin and F-actin.

Despite evidence that regulation of cofilin by phosphorylation is not required for vegetative growth in yeast, our data shed light on the mechanism of this regulation in other organisms. In principle, phosphorylation of Ser3 in vertebrate cells might inactivate cofilin/ADF by one of at least two different mechanisms. First, it is possible that the phosphate group at Ser3 could interact with positively charged residues that are essential for F-actin binding (e.g. Lys112 and Lys114 in porcine cofilin), thereby disrupting the cofilin–actin interaction. Alternatively, Ser3 itself could be positioned within a critical actin-binding sequence, and therefore the introduction of a phosphate group at this position would prevent this region from interacting with actin. Our data show that the N-terminal region of yeast cofilin is critical for both actin binding and depolymerization. The removal of this segment does not effect overall protein stability (as expected, since there is no precedent for a disordered protein terminus affecting a compact globular domain). Since conservation of the N-terminus of cofilin/ADF extends to yeast cofilin, which appears not to be phosphorylated, we suggest that the evolutionary conservation of this region reflects its importance in actin binding, rather than its role as a kinase/phosphatase recognition sequence. We further speculate that upon binding to actin, the cofilin N-terminus adopts a unique conformation, and that in more complex eukaryotes phosphorylation of Ser3 inhibits the interaction of this region with actin.

Table III. Positions of the mutations in yeast cofilin that impair F-actin binding alone (F), or both F-actin binding and G-actin binding (F/G)

Mutant	Residues	Secondary structure element
cof1-16 (F)	Arg80, Lys82	β5
cof1-17 (F/G)	Arg96, Lys98	α3
cof1-20 (F/G)	Asp123, Glu126	loop between β6 and α4
cof1-22 (F)	Glu134, Arg135, Arg138	α4
cof1-28 (F/G)	Met1–Gly5	disordered N-terminal region

Secondary structure elements are identified according to Fedorov *et al.* (1997).

Materials and methods

Plasmid construction

All DNA manipulations were performed by standard techniques (Ausubel *et al.*, 1990). Restriction endonucleases and other enzymes were obtained from New England Biolabs with the exception of calf alkaline phosphatase (Boehringer Mannheim) and *Taq*-polymerase (Ampli-Taq, Perkin Elmer). A 2.0 kb *COF1*-containing genomic *Eco*RI fragment was inserted into the *Eco*RI site of pRS315 to create plasmid pAM9. To be able to select for *COF1* integrations in yeast, we inserted an auxotrophic marker, *LEU2*, downstream from the *COF1* gene. Owing to the lack of useful restriction sites for this insertion, we created a *Spe*I site downstream of *COF1*. The *COF1* containing a *Bam*HI–*Sal*I fragment of pAM9 was subcloned to pALTER-1 (Promega) to create pPL3, and a *Spe*I restriction site was introduced 91 bp downstream from the end of the cofilin open-reading-frame using the PCR-based overlap extension method described by Higuchi *et al.* (1988). This plasmid was digested with *Sal*I and *Sac*I and the fragment carrying *COF1* was subcloned into the pBluescript® SK plasmid (Stratagene) digested with *Sal*I and *Sac*I to create pPL7. Plasmid pJJ250, carrying the *LEU2* gene (Jones and Prakash, 1990) was digested with *Pvu*II, and then *Spe*I adaptors (New England Biolabs) were ligated to the ends of the fragment carrying the *LEU2*. Both pPL7 and the *LEU2*-fragments were digested with *Spe*I, and they were ligated together to create pPL8. This plasmid contains the entire 2.0 kb *COF1* genomic fragment, with the *LEU2* gene inserted into the *Spe*I site 91 bp downstream from the end of the cofilin open-reading-frame in the same orientation as *COF1* (see Figure 1B). Site-directed *cof1* mutants were made in pPL8 by oligonucleotide-based mutagenesis (Transformer™ Clontech) following the method of Deng and Nickoloff (1992). The selection oligonucleotide (for definition see Deng and Nickoloff, 1992) used in the mutagenesis disrupts the unique *Eco*47III site located 930 bp downstream from the end of the *COF1* open-reading-frame.

To express yeast cofilin as GST–cofilin fusion proteins in *E.coli*, a genomic *COF1* DNA fragment was amplified by PCR using oligonucleotides that delete the intron close to the 5′ end and introduce *Bam*HI and *Eco*RI sites at the 5′ and 3′ ends, respectively. This fragment, which corresponds to a *COF1* cDNA, was ligated into a *Bam*HI–*Eco*RI digested pGEX2T plasmid (Ausubel *et al.*, 1990) to create plasmid pAM50. Site-directed mutations were introduced into this plasmid by oligonucleotide-based mutagenesis (Transformer™, Clontech) using a selection oligonucleotide which disrupts the unique *Bam*HI site in the pGEX2T polylinker without changing the amino acid sequence. In order to express a Met1–Gly5 deletion of Cof1p, a fragment lacking the codons for the five N-terminal amino acids of cofilin cDNA was amplified by PCR with oligonucleotides that create *Nco*I and *Hin*dIII sites at the 5′ and 3′ ends of the product, respectively. The fragment was digested with *Nco*I and *Hin*dIII and ligated into the pBAT4 vector (Peränen *et al.*, 1996) to create plasmid pPL45. As a control, the full-length yeast cofilin cDNA was also subcloned into the pBAT4 to create plasmid pPL44. All PCR constructs were sequenced by the chain-termination method and the clones containing undesired mutations were discarded. Mutations generated by oligonucleotide-based mutagenesis (Transformer™, Clontech) were confirmed by restriction endonuclease digestions and DNA sequencing.

Yeast strain construction

The cultivation and manipulation of yeast strains followed standard methods (Rose *et al.*, 1990). Yeast cell transformation was performed by the Li-acetate method (Ito *et al.*, 1983) and the strains were sporulated at 25°C in SPM medium as described by Kassir and Simchen (1991). Plasmids carrying the *COF1* or *cof1*-alleles linked to the *LEU2* auxotrophic marker were linearized by digestion with *Nco*I and *Bst*UI or *Nco*I and *Xho*I (the latter was carried out in the cases in which the site-directed mutations had created a *Bst*UI site in *COF1*). The DNA fragments carrying *COF1* or *cof1*-alleles were gel-purified and transformed into the strain DDY427, which is a *COF1/cofΔ1::HIS3* heterozygote (Moon *et al.*, 1993). The cells were plated on media selective for the *LEU2* auxotrophic marker and grown for 3 days at 25°C. The colonies were replica-plated onto selective media to identify transformants in which the gain of the *LEU2* marker was accompanied by the loss of the *HIS3* marker. Approximately 15% of the Leu^+ transformants were unable to grow on media selective for His^+. Cells from two such colonies were sporulated and six tetrads from each were dissected on YPD plates at 20°C. Cell suspensions of haploid segregants were spotted onto YPD agar at various temperatures and on appropriately supplemented SD agar to identify Leu^+ segregants. In order to confirm that these strains carry the correct *cof1* alleles, the *COF1* open-reading-frame was amplified from isolated genomic DNAs by PCR and the gel-purified DNA fragments were digested with the restriction endonucleases indicated in Table I. In order to confirm the correct chromosomal insertion of the *cof1* alleles, PCR analysis of genomic DNA was performed using two oligonucleotide primers, one of which is homologous to a site in the *LEU2* gene and the other which is homologous to a site outside of the integrated region.

Protein expression and purification

Wild-type and mutant yeast-cofilins were expressed as glutathione-*S*-transferase (GST) fusion proteins in *E.coli* JM109 cells under a control of the P_{lac} promoter. Cells were grown in 4000 ml of LB medium to an optical density of 0.5 at 600 nm, and expression was induced with isopropyl-thio-β-D-galactoside (IPTG, 0.4 mM). Cells were harvested 3 h after induction, washed with 50 ml of 20 mM Tris, pH 7.5, resuspended in 20 ml of PBS and lysed by sonication. GST fusion proteins were enriched using glutathione agarose beads as described by Ausubel *et al.* (1990). Cofilin–GST fusion proteins bound to glutathione–agarose-beads were incubated overnight with thrombin (0.05 mg/ml) to cleave cofilin away from GST. The beads were washed four times with 2 ml of 50 mM Tris pH 7.5, 150 mM NaCl. The supernatants were combined and concentrated in Centricon 10 kDa cut-off concentrators (Amicon Inc.) to 1 ml and loaded onto a Superdex-75 HiLoad gel-filtration column (Pharmacia Biotech) which had been equilibrated with 10 mM Tris pH 7.5, 50 mM NaCl. The peak fractions containing cofilin eluted at ~74 ml. These fractions were pooled, concentrated in Centricon 10 kDa tubes to a final protein concentration of ~100 μM, frozen in liquid N_2 and stored at –80°C. The N-terminal deletion (Cof1-28) and wild-type cofilin subcloned into pBAT4 were expressed as non-fusion proteins in *E.coli* BL21(DE3) cells (see Results for explanation). The cells were grown to an optical density of 0.5 at 600 nm, induced with 0.2 mM IPTG and harvested 3 h after induction. The cells were resuspended in 20 ml of 10 mM Tris pH 7.5, 0.15 mM PMSF, lysed by sonication and centrifuged for 30 min at 40 000 r.p.m. in a Ti45 rotor (Beckman Instruments). The supernatants were loaded onto a 50 ml Q-sepharose FF column (Pharmacia Biotech), equilibrated with 20 mM Tris pH 7.5, 0.15 mM phenylmethylsulfonyl fluoride (PMSF). A linear 0–1.0 M NaCl gradient developed over 200 ml was applied to the column. Peak fractions containing cofilin eluted at 0.4 M NaCl. These fractions were pooled and concentrated to 1 ml in Centricon 10 kDa cut-off devices. These samples were purified by gel-filtration on a Superdex-75 HiLoad column as described above. Yeast actin was purified as described previously (Buzan and Frieden, 1996). However, following treatment on the DNase I column the actin-containing fractions were precipitated with $(NH_4)_2SO_4$ and desalted into G-buffer (20 mM Tris pH 7.5, 0.2 mM ATP, 0.2 mM DTT, 0.2 mM $CaCl_2$) using G-25 columns (PD10, Pharmacia). Yeast actin was concentrated to a final concentration of 30 μM in Centricon 10 kDa cut-off devices, frozen in liquid N_2 and stored at –80°C.

Co-sedimentation assay

For actin filament co-sedimentation assays, 45 μl aliquots of 2.2, 4.4 or 6.6 μM yeast actin were polymerized in F-buffer (10 mM Tris pH 7.5, 0.7 mM ATP, 0.2 mM $CaCl_2$, 2 mM $MgCl_2$, 100 mM KCl and 0.2 mM DTT). After 60 min of polymerization, 5 μl of 20 μM cofilin or cofilin mutant proteins in F-buffer were mixed with F-actin samples and incubated at room temperature for 60 min. The actin filaments were sedimented by centrifugation at 90 000 r.p.m. for 20 min at 23°C in a TLA100 rotor (Beckman Instruments). Equal proportions of the supernatants and pellets were loaded on 12% SDS–polyacrylamide gels. The gels were Coomassie-stained and the intensity of actin and cofilin bands quantified using an IS-1000 densitometer (Alpha Innotech Corporation).

Depolymerization assay

For the F-actin depolymerization assay, 5 μM yeast actin was polymerized in F-buffer as described above. Five μl of F-actin were mixed with 40 μl of 0.6 μM cofilin (in F-buffer) in a quartz fluorometer cuvette with a 3 mm light path (Hellma). Actin filament depolymerization was followed by monitoring the decrease in light-scattering at 400 nm in a F-4010 fluorescence spectrophotometer (Hitachi). In order to reduce noise in the spectra, all solutions used for these experiments were clarified by centrifugation for 2 min, at 14 000 *g*.

Nucleotide exchange assay

The fluorescence signal provided by etheno-ATP (Molecular probes) bound to actin was used to measure the rate of nucleotide exchange of actin. Forty μl of G-buffer (10 mM Tris, 2 mM $CaCl_2$, 2 mM DTT,

25 μM ATP) with actin and cofilins (final concentrations of 2.5 μM and 0/2.5/5/7.5 μM, respectively) were mixed with 10 μl of 1 mM etheno-ATP and the reaction was followed in a F-4010 fluorescence spectrophotometer (Hitachi) at an exitation of 360 nm and emission of 410 nm.

Urea denaturation assays

Wild-type and mutant cofilins were used at final concentrations of 1–2 μM in 10 mM Tris, pH 7.5, 50 mM NaCl. The proteins were diluted into the appropriate concentration of buffered urea and incubated at room temperature for 1 h. Fluorescence measurements were carried out at an excitation of 280 nm and the emission was monitored at 355 nm. Normalized fluorescence was plotted against urea concentration to determine the mid-point of the unfolding transition.

Miscellaneous

Polyacrylamide gel electrophoresis in the presence of sodium dodecyl sulfate was carried out using the buffer system of Laemmli (1970). Native gel electrophoresis was performed as described earlier (Safer, 1989). Rhodamine–phalloidin staining was carried out as previously described (Lappalainen and Drubin, 1997). The protein concentrations were determined by using the calculated extinction coefficients for yeast cofilin at 280 nm ($\varepsilon = 15.9\ mM^{-1}\ cm^{-1}$) and for actin at 290 nm ($\varepsilon = 28.8\ mM^{-1}\ cm^{-1}$).

Acknowledgements

We thank Anne Moon for the yeast cofilin over-expression plasmid and Lisa Belmont and Bruce Goode for critical reading of the manuscript. We would also like to acknowledge Bruce Goode for his advice on site-directed mutagenesis. This work was supported by grants to D.G.D. from the National Institutes of General Medical Sciences (GM-42759) and the American Cancer Society (FRA-442) and to S.C.A. from the National Institutes of General Medical Sciences (GM-53807). P.L. was supported by long-term fellowships from the European Molecular Biology Organization and Human Frontier Science Program.

References

Abe,H., Obinata,T., Minamide,L.S. and Bamburg,J.R. (1996) *Xenopus laevis* actin-depolymerizing factor/cofilin: A phosphorylation-regulated protein essential for development. *J. Cell Biol.*, **132**, 871–885.

Agnew,B.J., Minamide,L.S. and Bamburg,J.R. (1995) Reactivation of phosphorylated actin depolymerizing factor and identification of the regulatory site. *J. Biol. Chem.*, **270**, 17582–17587.

Ausubel,F.M., Brent,R., Kingston,R.E., Moore,D.D., Seidman,J.G., Smith,J.A and Struhl,K. (1990) *Current Protocols in Molecular Biology.* John Wiley and Sons, New York.

Bamburg,J.R. and Bray,D. (1987) Distribution and cellular localization of actin depolymerizing factor. *J. Cell Biol.*, **105**, 2817–2825.

Bass,S.H., Mulkerrin,M.G. and Wells,J.A. (1991) A systematic mutational analysis of hormone-binding determinants in the human growth hormone receptor. *Proc. Natl Acad. Sci. USA*, **88**, 4498–4502.

Buzan,J.M. and Frieden,C. (1996) Yeast actin: Polymerization kinetic studies of wild type and a poorly polymerizing mutant. *Proc. Natl Acad. Sci. USA*, **93**, 91–95.

Carlier,M.F., Laurent,V., Santolini,J., Melki,R., Didry,D., Xia,G-X., Hong,Y., Chua,N.-H. and Pantaloni,D. (1997) Actin depolymerizing factor (ADF/cofilin) enhances the rate of filament turnover: implication in actin-based motility. *J. Cell Biol.*, **136**, 1307–1322.

Davidson,M.M.L. and Haslam,R.J. (1994) Dephosphorylation of cofilin in stimulated platelets: Roles for a GTP-binding protein and Ca^{2+}. *Biochem. J.*, **301**, 41–47.

Deng,W.P. and Nickoloff,J.A. (1992) Site-directed mutagenesis of virtually any plasmid by eliminating a unique site. *Anal. Biochem.*, **200**, 81–88.

Fedorov,A.A., Lappalainen,P., Fedorov,E.V., Drubin,D.G. and Almo,S.C. (1997) Structure determination of yeast cofilin. *Nature Struct. Biol.*, **4**, 366–369.

Gunsalus,K.C., Bonaccorsi,S., Williams,E., Verni,F., Gatti,M. and Goldberg,M.L. (1995) Mutations in *twinstar*, a *Drosophila* gene encoding a cofilin-ADF homologue, result in defects in centrosome migration and cytokinesis. *J. Cell Biol.*, **131**, 1243–1259.

Hatanaka,H., Ogura,K., Moriyama,M., Ichikawa,S., Yahara,I. and Inagaki,F. (1996) Tertiary structure of destrin and structural similarity between two actin-regulating protein families. *Cell*, **85**, 1047–1055.

Hawkins,M., Pope,B., Maciver,S.K. and Weeds,A.G. (1993) Human actin depolymerizing factor mediates a pH-sensitive destruction of actin filaments. *Biochemistry*, **32**, 9985–9993.

Hayden,S.M., Miller,P.S., Brauweiler,A. and Bamburg,J.R. (1993) Analysis of the interactions of actin depolymerizing factor with G- and F-actin. *Biochemistry*, **32**, 9994–10004.

Higuchi,R., Krummel,B. and Saiki,R.K. (1988) A general method of *in vitro* preparation and specific mutagenesis of DNA fragments: Study of protein and DNA interactions. *Nucleic Acids Res.*, **16**, 7351–7368.

Iida,K., Moriyama,K., Matsumoto,S., Kawasaki,H., Nishida,E. and Yahara,I. (1993) Isolation of a yeast essential gene, *COF1*, that encodes a homologue of mammalian cofilin, a low-M(r) actin-binding and depolymerizing protein. *Gene*, **124**, 115–120.

Ito,H., Fukuda,Y., Murata,K. and Kimura,A. (1983) Transformation of intact yeast cells treated with alkali cations. *J. Bacteriol.*, **153**, 163–168.

Janin,J., Miller,S. and Chothia,C. (1988) Surface, subunit interactions and interior of oligomeric proteins. *J. Mol. Biol.*, **204**, 155–164.

Jones,J.S. and Prakash,L. (1990) Yeast *Saccharomyces cerevisiae* selectable markers in pUC18 polylinkers. *Yeast*, **6**, 363–366.

Kassir,Y. and Simchen,G. (1991) Monitoring meiosis and sporulation in *Saccharomyces cerevisiae*. *Methods Enzymol.*, **194**, 94–110.

Laemmli,U.K. (1970) Cleavage of structural proteins during the assembly of the head bacteriophage T4. *Nature*, **227**, 680–685.

Lappalainen,P. and Drubin,D.G. (1997) Cofilin promotes rapid actin filament turnover *in vivo*. *Nature*, **388**, 78–82.

Leonard,S., Gittis,A., Petrella,E., Pollard,T. and Lattman,E. (1997) Crystal structure of the actin-binding protein actophorin from *Acanthamoeba*. *Nature Struct. Biol.*, **4**, 369–373.

McKim,K.S., Matheson,C., Marra,M.A., Wakarchuk,M.F. and Baillie, D.L. (1994) The *Caenorhabditis elegans unc-60* gene encodes protein homologous to a family of actin binding proteins. *Mol. Gen. Genet.*, **242**, 346–357.

McLaughlin,P.J., Gooch,J.T., Mannherz,H.G. and Weeds,A.G. (1993) Structure of gelsolin segment 1 actin complex and the mechanism of filament severing. *Nature*, **364**, 685–692.

Moon,A. and Drubin,D.G. (1995) The ADF-cofilin proteins: Stimulus-responsive modulators of actin dynamics. *Mol. Biol. Cell*, **6**, 1423–1431.

Moon,A.L., Janmey,P.A., Louie,K.A. and Drubin,D.G. (1993b) Cofilin is an essential component of the yeast cortical cytoskeleton. *J. Cell Biol.*, **120**, 421–435.

Morgan,T.E., Lockerbie,R.O., Minamide,L.S., Browning,M.D. and Bamburg,J.R. (1993) Isolation and characterization of a regulated form of actin depolymerizing factor. *J. Cell Biol.*, **122**, 623–633.

Moriyama,K., Yonezawa,N., Sakai,H., Yahara,I. and Nishida,E. (1992) Mutational analysis of an actin-binding site of cofilin and characterization of chimeric proteins between cofilin and destrin. *J. Biol. Chem.*, **267**, 7240–7244.

Nagaoka,R., Abe,H., Kusano,K.I. and Obinata,T. (1995) Concentration of cofilin, a small actin-binding protein, at the cleavage furrow during cytokinesis. *Cell Motil. Cytoskeleton*, **30**, 1–7.

Ogawa,K., Tashima,M., Yumoto,Y., Okuda,T., Sawada,H. and Maruyama,Y. (1990) Coding sequence of human placenta cofilin complementary DNA. *Nucleic Acids Res.*, **18**, 7169.

Peränen,J., Rikkonen,M., Hyvönen,M. and Kääriäinen,L. (1996) T7 vectors with a modified T7lac promoter for expression of proteins in *Escherichia coli*. *Anal. Biochem.*, **236**, 371–373.

Pollard,T.D. (1986) Rate constants for the reactions of ATP- and ADP-actin with the ends of actin filaments. *J. Cell Biol.*, **103**, 2747–2754.

Reijo,R.A., Cooper,E.M., Beagle,G.J. and Huffaker,T.C. (1994) Systematic mutational analysis of the yeast beta-tubulin gene. *Mol. Biol. Cell*, **5**, 29–43.

Rose,M.D., Winston,F. and Hieter,P. (1990) *Methods in Yeast Genetics: A Laboratory Course Manual*, Cold Spring Harbor Laboratory Press, NY, USA.

Rosenblatt,J., Agnew,B.J., Abe,H., Bamburg,J.R. and Mitchison,T.J. (1997) *Xenopus* Actin Depolymerizing Factor/Cofilin XAC is responsible for the turnover of actin filaments in *Listeria monocytogenes* tails. *J. Cell Biol.*, **136**, 1323–1332.

Safer,D. (1989) An electrophoretic procedure for detecting proteins that bind actin monomers. *Anal. Biochem.*, **178**, 32–37.

Saito,T., Lamy,F., Roger,P.P., Lecocq,R. and Dumont,J.E. (1994) Characterization and identification of cofilin and destrin as two thyrotropin- and phorbol ester-regulated phosphoproteins in thyroid cells. *Exp. Cell Res.*, **212**, 49–61.

Samstag,Y., Dreizler,E.M., Ambach,A., Sczakiel,G. and Meuer,S.C. (1996) Inhibition of constitutive serine phosphatase activity in T lymphoma cells results in phosphorylation of pp19-cofilin and induces apoptosis. *J. Immunol.*, **156**, 4167–4173.

Sutoh,K. and Mabuchi,I. (1989) End-label fingerprintings show that an N-terminal segment of depactin participates in interaction with actin. *Biochemistry*, **28**, 102–106.

Theriot,J.A. and Mitchison,T.J. (1991) Actin microfilament dynamics in locomoting cells. *Nature*, **352**, 126–131.

Theriot,J.A., Mitchison,T.J., Tilney,L.G. and Portnoy,D.A. (1992) The rate of actin-based motility of intracellular *Listeria monocytogenes* equals the rate of actin polymerization. *Nature*, **357**, 257–260.

Weeds,A. and Maciver,S. (1993) F-actin capping proteins. *Curr. Opin. Cell Biol.*, **5**, 63–69.

Wertman,K.F., Drubin,D.G. and Botstein,D. (1992) Systematic mutational analysis of the yeast ACT1 gene. *Genetics*, **132**, 337–350.

Yonezawa,N., Nishida,E. and Sakai,H. (1985) pH control of actin polymerization by cofilin. *J. Biol. Chem.*, **260**, 14410–14412.

Yonezawa,N., Nishida,E., Koyasu,S., Maekawa,S., Ohta,Y., Yahara,I. and Sakai,H. (1987) Distribution among tissues and intracellular localization of cofilin, a 21kDa actin-binding protein. *Cell Struct. Funct.*, **12**, 443–452.

Yonezawa,N., Nishida,E., Iida,K., Yahara,I. and Sakai,H. (1989a) Studies on interaction of cofilin with actin: Effects of phosphoinositides and analyses of the actin-binding site. *Cell Struct. Funct.*, **14**, 892.

Yonezawa,N., Nishida,E., Ohba,M., Seki,M., Kumagai,H. and Sakai,H. (1989b) An actin-interacting heptapeptide in the cofilin sequence. *Eur. J. Biochem.*, **183**, 235–238.

Yonezawa,N., Homma,Y., Yahara,I., Sakai,H. and Nishida,E. (1991) A short sequence responsible for both phosphoinositide binding and actin binding activities of cofilin. *J. Biol. Chem.*, **266**, 17218–17221.

Received March 27, 1997; revised June 9, 1997